

Investigation of Within-Tablet Dynamics for Extended Release of a Poorly Soluble Basic Drug from Hydrophilic Matrix Tablets Using ATR-FTIR Imaging

ZAHOOR, F.D. <<http://orcid.org/0000-0003-1462-0983>>, MADER, K.T., TIMMINS, P. <<http://orcid.org/0000-0002-5840-0678>>, BROWN, J. and SAMMON, Chris <<http://orcid.org/0000-0003-1714-1726>>

Available from Sheffield Hallam University Research Archive (SHURA) at:

<https://shura.shu.ac.uk/28227/>

This document is the Accepted Version [AM]

Citation:

ZAHOOR, F.D., MADER, K.T., TIMMINS, P., BROWN, J. and SAMMON, Chris (2020). Investigation of Within-Tablet Dynamics for Extended Release of a Poorly Soluble Basic Drug from Hydrophilic Matrix Tablets Using ATR-FTIR Imaging. *Molecular Pharmaceutics*, 17 (4), 1090-1099. [Article]

Copyright and re-use policy

See <http://shura.shu.ac.uk/information.html>

Investigation of within-tablet dynamics for extended release of a poorly-soluble basic drug from hydrophilic matrix tablets using ATR-FTIR imaging

Farah Deeba Zahoor^a, Kerstin Mader^a, Peter Timmins^c, Jonathan Brown^d, Chris Sammon^{a*}

^aSheffield Hallam University, City Campus, Howard Street, Sheffield, S1 1WB, UK,

^cUniversity of Huddersfield, Queensgate, Huddersfield HD1 3DH, UK, ^dBristol-Myers Squibb, Moreton Merseyside CH46 1QW, UK

*Corresponding author.

Tel.: +44 114 2253069

E-mail: c.sammon@shu.ac.uk

Abstract

Hydrophilic matrices are an effective option for oral controlled release but can face challenges in terms of bioavailability and efficacy when used in conjunction with poorly-soluble, weakly basic drugs. Attenuated total reflectance Fourier transform infrared (ATR-FTIR) imaging provides dynamic information relating to the location and chemical nature of both the sustained release matrix and the active pharmaceutical ingredient (API) during hydration/dissolution. In this study we have identified a model system combining itraconazole (IT), a poorly-soluble, weakly basic API that has a pKa in the physiological range, and hydroxypropyl methylcellulose (HPMC) which is a commonly used oral tablet matrix. This system was investigated to determine swelling kinetics at different pH at a fixed ionic strength and to facilitate the study of the influence of hydrating media pH on drug particle movement (translocation).

Using ATR-FTIR imaging we were able to show that gel layer formation and swelling were independent of pH but highly dependent on the ionic strength of the hydrating medium in placebo tablets. When the ionic strength was fixed, gel layer formation and radial swelling were both shown to be pH dependent when IT was incorporated into the matrix. This was verified using optical imaging.

The chemical specificity of ATR-FTIR imaging permitted the observation of transformational changes of IT from free base to the ionised form in the tablet core during hydration. This phenomenon was shown to be greater at pH 1.5 than pH 7.

ATR-FTIR imaging was able to follow drug particle translocation at both pH 1.5 and pH 7, however, the extent of migration away from the tablet core was shown to be greater at lower pH. The location of the translocated particles within the gel layer was different between the two studied pHs with particles being located close to the erosion front at pH 7 and within the diffusion front at pH 1.5. In both pH environments translocated IT particles were shown to be predominantly in the free base form. No evidence of fully solubilised IT was observed in the surrounding medium due to the inherent aqueous solubility of IT being below the instrument detection limits.

This work highlighted the value of utilising a chemically specific spectroscopic tool to increase the understanding of the nature of factors affecting the release of a pH-dependent, poorly-soluble drug from a hydrophilic matrix at different pH and permitted greater insight into what happens inside the polymer matrix during drug release.

Key Words

Real time imaging, poorly-soluble drug, itraconazole, gel layer, HPMC, extended release

1. Introduction

Hydrophilic matrix tablets based on hydroxypropyl methylcellulose (hypromellose, HPMC) are a favourable choice for oral extended drug release dosage forms for a number of reasons including the knowledge base for the technology, regulatory status, low cost of rate control polymer, ease of manufacture and relative inertness [1]. In contact with water, HPMC rapidly undergoes hydration and swelling with the formation of a gel layer, a dynamic 'shell' around the tablet core. The extent of the hydrated polymer increases through ingress of fluid into the tablet over time and contributes to controlling the release of the drug by modulating the rate of water ingress [2]. Drug dissolution in, and diffusion through, the matrix as well as erosion of the hydrated polymer under shear at the interface between the gel layer and the bulk medium also are processes that contribute to drug release. Understanding the mechanisms controlling rate of drug release from an HPMC hydrophilic matrix tablet can be pursued by considering the movement of three fronts inside the evolving matrix tablet over time (Fig. 1a) : the boundary between yet-to-be hydrated polymer and hydrated polymer (swelling front); between hydrated polymer and bulk aqueous medium (erosion front); within the hydrated gel where undissolved drug is in equilibrium with dissolved drug (diffusion front) [1] [3]. The presence of solid undissolved drug particles in the hydrated gel layer can impair the swelling of the polymer matrix by restricting the disentanglement of the polymer chains, which may be an important parameter in the case of poorly water-soluble compounds with marked pH-dependent solubility. There is also a correlation between poor drug solubility and erosion of the matrix [4]. For poorly-soluble drugs in hydrophilic matrices, the erosion mechanism of the hydrated polymer is important as it is this erosion that results in the liberation of undissolved drug [4].

Previous studies have incorporated non-diffusing insoluble markers to gain insight and quantify swelling within the gel layer of hydrophilic matrix tablets (HPMC). The movement of the fluorescent markers was tracked and observed using a confocal laser scanning microscope [5]. Interestingly, analysis of the tracks indicated a wave of expansion that started and was greatest at the exterior, moving towards the core. The findings also suggested that as deeper layers started to expand, swelling continued in the outer layers.

HPMC is chemically stable over the physiological pH range [6] however, the swelling properties of HPMC are strongly influenced by the ionic strength of the medium [7] [8]. The ionic strength can vary considerably in the fluid within the gastrointestinal tract and depending on fasted and fed states, can range from 0-0.5 mol/L, impacting on drug release from a hydrophilic polymer matrix [7]. Many different approaches have been used to investigate the formation of the hydrated gel layer and the impact of ionic strength employing a range of techniques [9] [10]. Bajwa *et al.* used real-time confocal fluorescence imaging to investigate movement and migration of the early stages of HPMC gel layer formation using the fluorophore Congo red, which selectively binds with the cellulosic unit and hence acts as a marker for the hydrated HPMC [8]. The authors concluded that gel layer growth was suppressed with increasing salt concentration of the hydration medium.

Poorly-soluble ionisable drugs will exhibit different dissolution behaviour within the physiological pH range. Weakly basic compounds exhibit a marked increase in solubility at low pH while being practically insoluble at neutral pH [2] [11]. A significant number of new drugs in development fall into this category [12], although the phenomenon may be ameliorated to a degree by incorporating pH-modifiers within the matrix to yield improved *in vivo* performance [13]. A further method to achieve an improved oral bioavailability is by the creation of a water-soluble salt form of the weakly basic drug [14].

FTIR imaging enables multiple spectra to be collected simultaneously, allowing a chemical image of the material to be generated relatively quickly [15] [16] [17]. From this, information about the polymer, drug and water distribution can be gained simultaneously. The advantage of this approach is the ability to provide characterisation of the molecular species present and morphology of the polymer matrix [16]. FTIR images consist of spectral and spatial information and therefore require additional steps for converting the data into chemically and physically significant information. There are several methodologies for doing this, the simplest involves plotting the peak height or peak area of a band from a known component.

ATR-FTIR imaging has previously been used to study the mechanism of drug release from HPMC matrices. [18] [19] [20]. Work by van der Weerd and Kazarian described an approach to studying drug release from a tablet by using a combination of chemical imaging via ATR-FTIR imaging and dissolution. Niacinamide incorporated into a HPMC matrix was used as a model system [21]. Using a partial least squares regression (PLS) calibration, quantitative analysis for the concentration of water, polymer and drug as a function of time was possible.

Hifumi *et al* have used ATR-FTIR imaging to investigate the influence of different polymer matrices on drug release. They studied ibuprofen loaded HPMC films as a rapid release model and ibuprofen loaded polyvinylpyrrolidone (PVP) films for extended release. By controlling the local pH by incorporating a pH modifier and ionic strength around the HPMC via a hydrophobicity modifier, drug release behaviour could be controlled [22].

Ewing *et al* used ATR-FTIR imaging combined with a polydimethylsiloxane microfluidic device to monitor the behaviour and release of ibuprofen *in situ* under flowing conditions at pH 1 and 7. It was reported that the low pH environment inhibited the release of the drug due to conversion from the molecularly dispersed ibuprofen to the crystalline form [23].

The aim of the current study was to use a poorly water-soluble, weakly basic and lipophilic model drug system to develop an insight how these types of drugs behave within the tablet matrix. We have selected itraconazole (IT) as the chosen model drug as although it is not a candidate for oral extended delivery from a hydrophilic matrix system it met the stated criteria for a suitable model compound for this work in that it exhibits pH-dependent and poor solubility, close to 1 ng/mL at pH 7 and 4 µg/mL at pH 1 [24], with a pKa of 3.7. This is well inside the physiological pH range and characteristic of the most challenging compounds which might be considered for delivery from hydrophilic matrix systems. It also is very amenable to the spectroscopic imaging approaches we have applied in this work. As a basis for future work, in this exploration of the behaviour of IT within the hydrating matrix, the methodology adopted permitted an opportunity to gain an insight into how such drugs behave both as environmental pH changes and in the absence of a pH modifier within the matrix.

This study has used ATR-FTIR imaging to monitor the hydration of the polymer and migration of the drug in the diffusion front over time and examined the influence of ionic strength on the formation of the HPMC gel layer. ATR-FTIR imaging allowed dissolution to be studied in real-time, mapping both the location of the drug and its chemical characteristics (e.g. ionisation state) as it dissolved. The behaviour of salt forms of a drug within polymeric systems has been characterised previously. However, the combined assessment of poor solubility, very weakly basic drug and excipients and water in a formulation undergoing dynamic changes including ionisation, dissolution, hydration, swelling, particle dislocation with a view to informing future product design has not been reported [23]. The application of this approach will permit a greater understanding of the factors controlling drug release and enable a more effective quality-by-design approach to formulating HPMC matrix tablets.

2. Materials and methods

2.1 Materials

Itraconazole (99% Acros Organics) and HPMC (grade Methocel®K100M CR Premium grade) powders were used as received. For the hydration studies two different hydrating media were used to investigate pH effects; 0.1 M HCl solution (pH 1.5) and tris(hydroxymethyl)aminomethane hydrochloride buffer solution (tris buffer, purchased from Sigma Aldrich, molecular biology grade pH 7.2). In order to explore the influence of ionic strength on the hydration of the HPMC two different ionic strength solutions were investigated. In order to minimise Hofmeister series-like effects, ionic strength was managed by using monovalent buffering agents [25]. The 0.1 M HCl was prepared by diluting concentrated HCl 37% with deionised water having a resistivity of 18.2 MΩ. For the low ionic strength tris buffer, a 0.1 M solution was prepared by carrying a 10-fold dilution of the as-received solution. In order to obtain the high ionic strength solutions a 1 M concentration was used. For the 1 M tris solution, the as-received buffer was used. For the high ionic strength solution at low pH, sodium chloride (general purpose grade, Fischer Scientific) was added to the 0.1 N HCl solution to increase the ionic strength to 1 M.

2.2 Preparation and Characterisation of Tablets

HPMC tablets containing 20% w/w itraconazole were prepared by tumble blending (Stuart STR4 rotator drive) for 5 hours at approximately 30 rpm. Flat-faced matrix tablets (10 mm) containing 90 mg total powder were manufactured by direct compression on a Specac Atlas Manual press (Specac, Orpington, UK) using a compaction pressure of 625 MPa and a 5 minute compaction time. The average IT content (n=6) was determined using Near Infrared (NIR) and shown to be 19.37% w/w with a uniform distribution across the tablet as determined by Raman microscopy (supporting information S_Fig.1 and S_Fig.2). The advantages of using Raman microscopy rather than ATR-FTIR imaging to determine content uniformity of an API include enhanced spatial resolution, the possibility of achieving spot sizes less than 2 µm, the ability to map larger areas [26] (the mid-IR ATR method is limited to a fields of view ~640x640 µm² in our system) and easier discrimination of an aromatic API in an HPMC matrix.

2.3 In vitro release studies

Dissolution studies were carried out using Agilent 708 on the 20% w/w IT formulation (n=6) in 900 ml of 0.1N HCL and 0.1M tris buffer using the USP Type-II method. A paddle speed of 75 rpm and a temperature of 37±0.5 °C was used in all experiments [27]. A 5 ml aliquot was withdrawn at different time intervals and assayed for IT using ultraviolet–visible spectroscopy (Agilent Cary 60) by measuring the absorbance at 257 nm.

2.4 Collection of ATR-FTIR images

Mid-IR spectroscopic images were collected using a Varian 680-IR spectrometer (Agilent Technologies LDA UK Limited, Stockport, UK) coupled to a variable temperature Golden Gate single reflection ATR sampling accessory (Specac, Orpington, UK) held at 37°C. Images were collected at a spectral resolution of 8 cm⁻¹ with 8 co-additions. It was observed that an S/N advantage can be obtained by using a large number of background scans whilst maintaining the speed advantage of having fewer sample scans. Therefore, blank ATR crystal images at

a resolution of 8 cm^{-1} and 256 co-additions were used as a background reference for image processing.

2.5 Hydration Experiments using ATR- FTIR Imaging

Hydration studies on the tablets were performed as follows and shown schematically in Fig 1. Each tablet was placed on the ATR crystal such that approximately one-third of the ATR crystal surface was covered. Pressure was then applied to the tablet using a sapphire anvil and a good optical contact between the sample and the ATR crystal was confirmed by checking the quality of the image of the dry tablet, this limited swelling in the axial direction. A polyester ring, of larger diameter than the tablet itself to permit unimpeded radial expansion, was sealed around the tablet and 5 ml of sonicated pH 7 tris buffer or 0.1 N (pH 1.5) HCl (37°C) was carefully added from one side of the crystal as hydrating medium.

Hydration was studied over a 3 hour period at a temperature of 37°C , images were collected every 2 min for the first 10 min, every 10 min over the following 70 min and every 20 min for the remainder of the experiment. Chemical images for each component in the system were generated by plotting the peak area of the 1630 , 1510 and 1041 cm^{-1} bands to show the distribution of water, IT and HPMC respectively using ISys 5.0 chemical imaging software (Malvern Instruments, Malvern, UK).

It should be noted that this experimental arrangement permits only observation of swelling and water ingress, particle translocation if it occurs and dissolution/diffusion of the drug in the hydrated matrix. It is not capable of monitoring erosion due to the low shear environment that exists within the cell. However, this is not considered to be a limitation in this context as it still allows assessment of within-tablet dynamics due to hydration and swelling at pH values within the tablet where drug will be insoluble (high pH medium) or have some solubility (low pH medium).

2.6 Optical Imaging to determine to radial and axial swelling

Optical images of the axial and radial swelling were collected using two Canon 5D MK3 digital cameras equipped with 100mm macro lenses, arranged to capture axial and radial images of the tablets simultaneously. Images were obtained from the HPMC placebo and the 20% w/w IT loaded HPMC formulation in dissolution media at pH 1.5 and 7 ($n=6$). The tablets were placed onto a 3-prong sample holder located in a glass cell and 40 ml of either 0.1N HCL or 0.1M tris buffer was added. Images were collected at 5 minute intervals for a period of 180 minutes. Data analysis was conducted using image analysis software (ImageJ 1.52a) to determine to the area change in both the axial and radial dimensions. Dimensional changes of the drug loaded tablets immersed in media at the two different pHs were statistically compared using a two-way analysis of variance (ANOVA) to determine the statistical significance of any differences (Prism V 7.03).

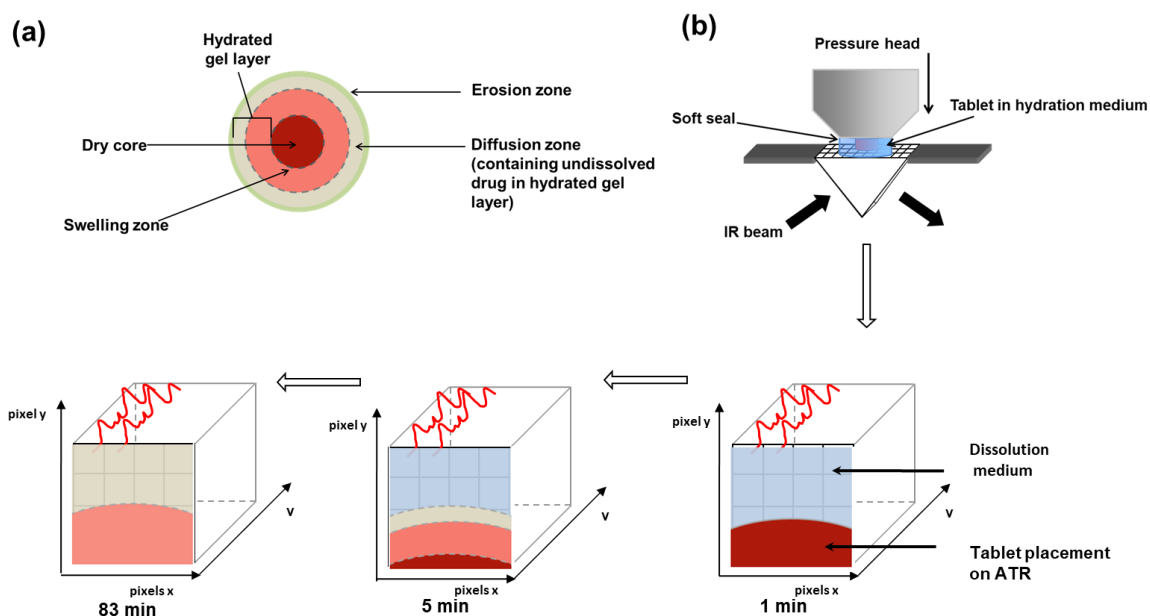


Fig. 1a: Schematic of different fronts of a hydrating hydrophilic tablet, looking down onto the upper tablet surface as if one could see through it, highlighting dry core, swelling, diffusion and erosion fronts, adapted from Timmins *et al.* reproduced with permission from Therapeutic Delivery as agreed by Newlands Press Ltd [1]. (b): Schematic of ATR-FTIR imaging set-up over the course of the hydration period using a Focal Plane Array (FPA) detector.

3.0 Results and Discussion

3.1 *In vitro* release studies

Dissolution profiles obtained for the 20% w/w IT loaded tablets (S_Fig 3) showed a marked difference in release rate between the two pHs. At pH 1.5 sustained release of IT was observed over the 24h experiment, although when the experiment was stopped at this point, only 24% of the contained IT had been released. In contrast, the same IT tablets in the pH 7 medium showed release to be <1% at 24 hours. There was no evidence of burst release during these measurements at either pH for this API/polymer matrix. However, the results showed clear evidence of an increase in both dissolution rate and percentage IT release (associated with increased solubility of IT) in the pH 1.5 medium, as anticipated and in full agreement with previous studies [28].

3.2 ATR-FTIR Imaging of reference materials

Reference spectra for IT, HPMC, 0.1 N HCl and tris buffer were generated by calculating the mean of the spectra obtained from a single image obtained as described in 2.4.

Spectral profiles were generated from the average of ATR-FTIR images obtained of the reference materials and were used to identify species specific bands from which it was possible to generate chemical images (Fig 2). The bands of interest were shown to be the $\delta(\text{OH}) \sim 1620 \text{ cm}^{-1}$ for water (used as a marker for tris buffer and 0.1 N HCl, due to water being

the main component), $\nu(\text{C-O}) \sim 1041 \text{ cm}^{-1}$ for HPMC and aromatic $\nu(\text{C=C}) \sim 1510 \text{ cm}^{-1}$ for the total IT distribution.

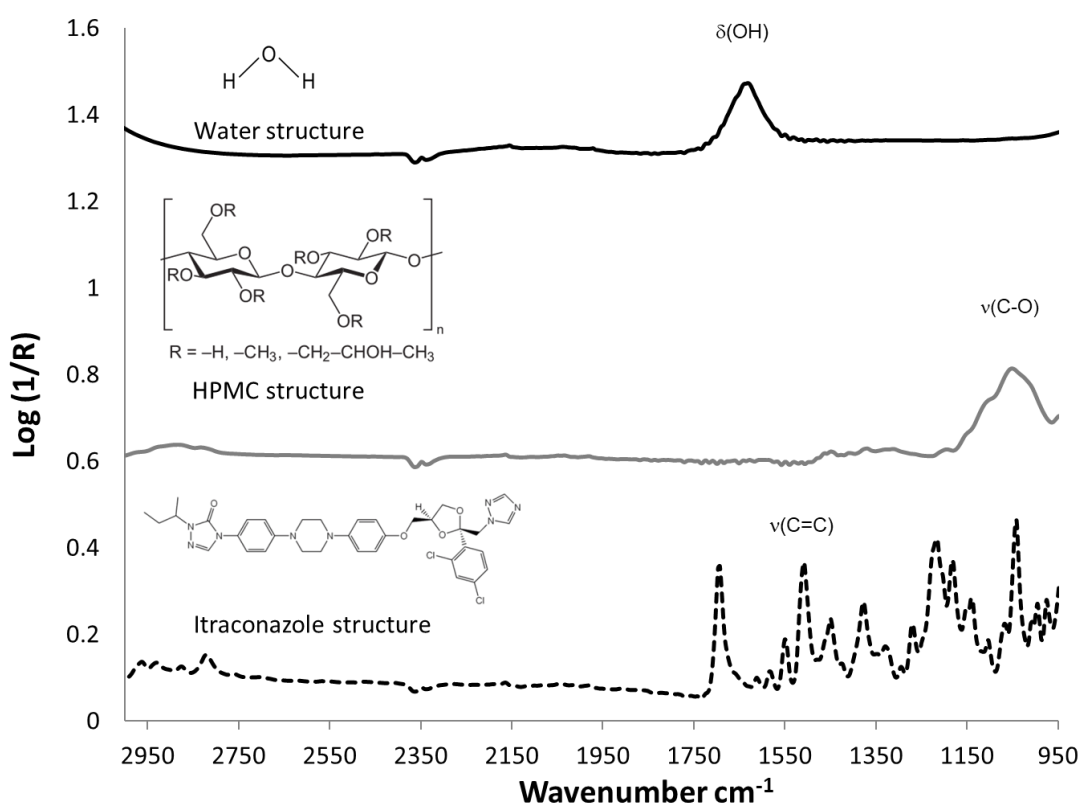


Fig. 2: Average ATR-FTIR imaging spectra obtained from reference materials, highlighting $\delta(\text{OH})$, $\nu(\text{C-O})$ and $\nu(\text{C=C})$ in water, HPMC and IT respectively. Highlighted bands used for peak area integration for images to show distribution of water, IT and HPMC.

3.3 ATR-FTIR Imaging of HPMC tablets

Mid-IR images of matrix tablet composed simply of HPMC hydrating at pH 1.5 and 7 using low and high ionic strength media over the 3 hour hydration period were generated using the bands identified in section 3.2 and show the evolution of the ingress of water into the tablet matrix and the growth of the gel layer. (Fig. 3). High intensity regions are coloured red, while low intensity regions are blue. Increasing intensity is denoted by the numerical values on the accompanying colour scale bars.

From the water distribution images (Fig. 3a) it is evident that water ingress occurs rapidly and full penetration throughout the tablet, visible within the field of view, occurs by around 19 minutes irrespective of the pH or ionic strength environment. HPMC distribution images show the (non-hydrated) tablet core is located towards the lower half of the images (Fig. 3b). The intensity of this dark red/yellow HPMC distribution in the high ionic strength medium at pH 1.5

and 7 (Fig. 3b (iii) and (iv)) is far greater throughout the duration of the experiment in comparison to the low ionic strength images (Fig. 3b(i) and (ii)).

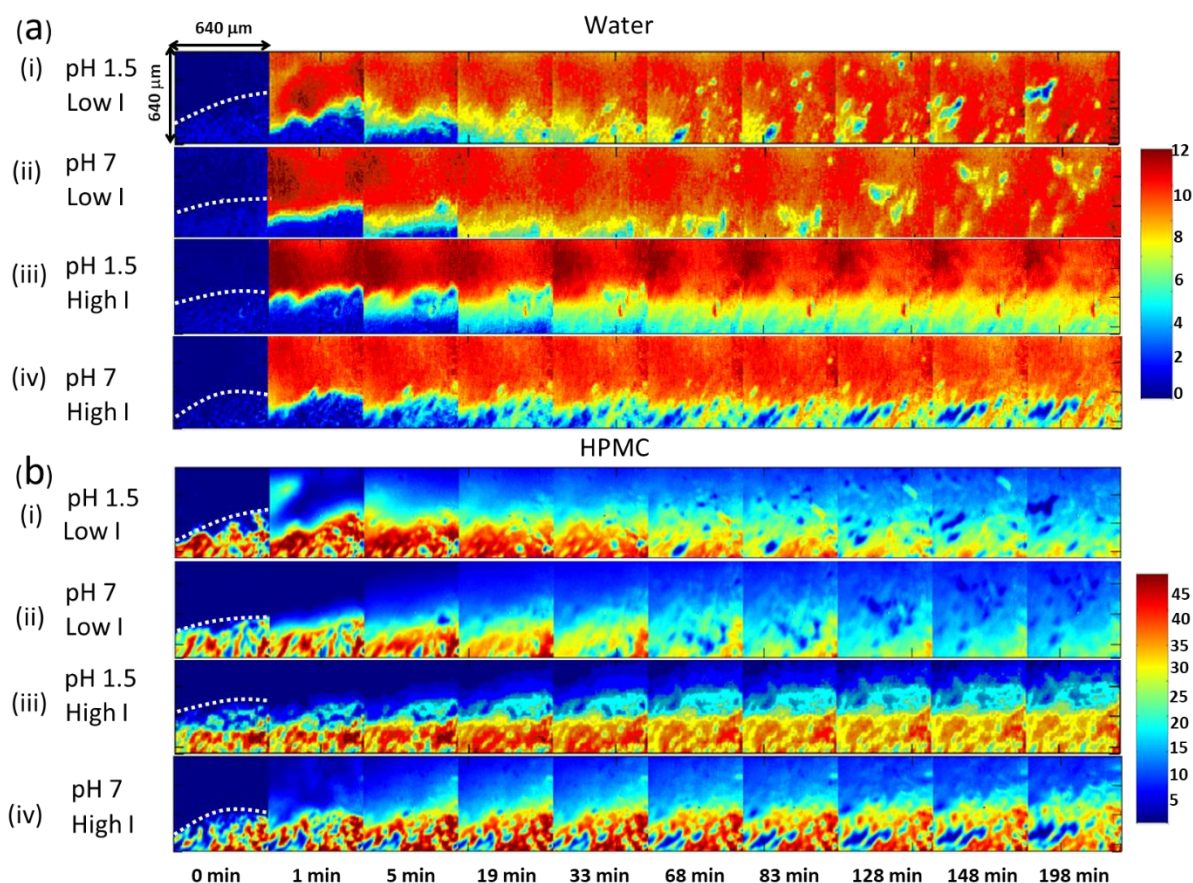


Fig. 3: Selected ATR-FTIR images were collected over the time course of hydration experiments for placebo tablets in low and high ionic strength solutions at pH 1.5 and pH 7 showing (a) water and (b) HPMC distribution. Images were generated using methods described in section 2.5. The dotted lines in the first column of images denotes the boundary between the tablet and air/water.

To gain an insight into the gel layer behaviour, the peak area ratio of the $\nu(\text{C-O})$ in the HPMC and the $\delta(\text{OH})$ for water was plotted. The gel layer was defined as the cyan zone corresponding to values between 2.2 and 3.8, on the colour scale shown in Fig. 4 and consisted of a combination of water and polymer at varying concentrations. Fig. 4a and b clearly highlight the rapid formation of the gel layer at pH 1.5 and pH 7 in a low ionic strength environment. The dark red colour corresponded to regions with high polymer content. Conversely, regions of hydrated HPMC with increasing water content are denoted by the yellow, green and cyan zones respectively.

The gel layer behaviour is the same between the different pH environments for the pure HPMC with the same ionic strength (Fig 4). For the low ionic strength media (Fig. 4a and 4b), at both pH, initial swelling is observed from the 1 minute time point. The dry core diminishes rapidly and the gel layer recedes towards the edge of the field of view within the time frame of the experiment.

For the high ionic strength images at pH 1.5 and 7, swelling is observed from the outset the gel layer is much more stable over the duration of the experiment (Fig. 4c and d). Thus confirming the ionic strength of the media had a significant impact on the gel layer behaviour. This is consistent with previous studies looking at the impact of ionic strength and HPMC gel formation [6] [8] [10], where the gel layer behaviour is shown to be independent of pH but highly dependent on the ionic strength of the medium. At higher ionic strength, less effective penetration of the water into the core and development of hydrated, swollen polymer gel layer is observed.

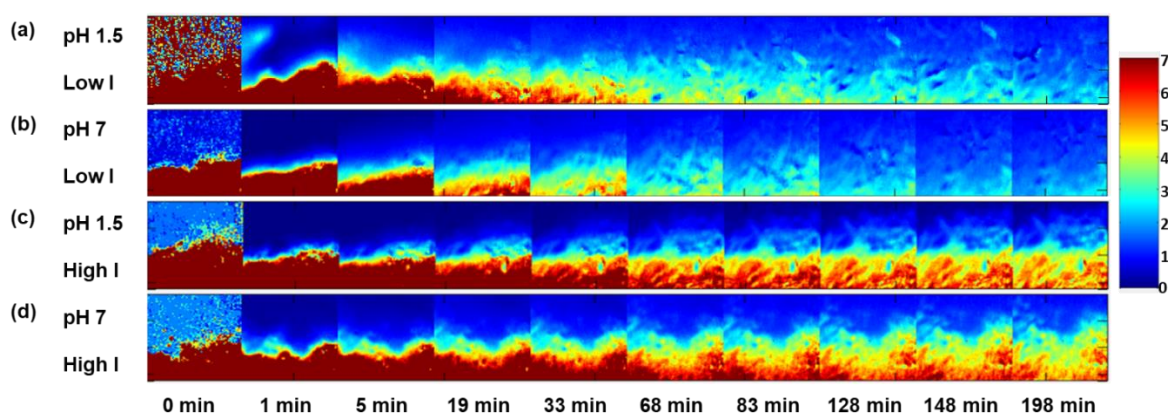


Fig. 4: ATR-FTIR images of HPMC/water peak area ratio images over hydration period, showing HPMC gel layer evolution for (a) pH 1.5 and (b) pH 7 low ionic strength solutions. (c) pH 1.5 and (d) pH 7 high ionic strength solutions.

3.4 FTIR imaging hydration experiments on pure 20% w/w IT loaded tablets

To determine the influence of pH on IT-containing matrices, the ionic strength of the hydration medium was matched whilst the pH was modified. The strategy adopted was to use the low ionic strength medium as described in Section 3.3, thereby ensuring that any changes observed to the drug could be attributed to the pH environment alone.

Fig. 5 shows the results of the ATR-FTIR imaging hydration experiments performed on 20% w/w IT-loaded tablets hydrated with a low ionic strength medium (0.1 mol/L) at pH 1.5 and 7.

Fig. 5a, 5b and 5c show the water, HPMC distribution and gel layer evolution over the timeframe of the experiment. These results are similar to those observed with the IT-free HPMC tablets in a low ionic strength medium, shown in Figs. 3 and 4. However, interrogation of the gel layer images shown Fig. 5c over the hydration period appears to show visible differences between the swelling behaviour in the two pH environments.

The distribution and dispersion of the total IT over the hydration period (Fig. 5d) differs dramatically between the two pH environments. At pH 7, an environment where the drug is very insoluble, the matrix expands and swells, taking some drug particles with it but the drug predominantly remains in the core and is not readily able to dissolve or disperse into the hydrating matrix, reflecting the *in vitro* dissolution data. However, at pH 1.5, as the HPMC matrix expands and swells the IT shows enhanced mobility and moves with the apparent diffusion front, which has improved definition and has more inherent structure at this pH. At pH 7 the diffusion front and the swelling front are likely to be almost coincident. As indicated previously, the solubility of IT is very different in the two pH environments. We hypothesise that the additional structure within the diffusion front, evident at pH 1.5, is related to the pH-dependent solubility of IT [24] [29]. This has the potential to impact on the mechanism drug release kinetics [30] [31].

The FTIR imaging data confirms that the HPMC swelling is similar at each pH for the placebo but is measurably different when IT is incorporated into the tablet. This suggests the possibility of an additional mechanism affecting drug release kinetics beyond pH enabled drug solubility in the hydrated matrix. To explore this further and to inform the findings observed from the ATR-FTIR imaging, a program of work to determine the swelling kinetics of IT loaded tablets was conducted using optical imaging (see section 3.7).

Evidence of undissolved IT particle movement was observed in both pH environments. This phenomenon of drug particle translocation has previously been studied using optical methods [4]. Using ATR-FTIR imaging, as the HPMC matrix swells and expands, undissolved drug particles moving outward in the expanding hydrated gel layer can be followed without the need for other markers, such as dyes or glass beads [8], advantageously it is possible to also confirm the chemical form of the drug as the particle is moving.

Expanding the diffusion front area of images at selected time point permits the exploration of the translocation of the IT particles in more detail (Fig 6). In these enlarged images, it is possible to identify and track individual particles, an example of a tracked particle is highlighted at both pH 1.5 (Fig 6a) and pH 7 (Fig 6b) images. At each time point, the change in the position of the interface between the IT rich area and the surrounding medium was calculated. This was then subtracted from the measured distance of particles relative to their original position giving a measure of the relative movement of the particle and interface at each time point.

Five particles were tracked from the pH 1.5 and 7 datasets and their movement is plotted in Fig 6c. It should be noted that due to the limited field of view of the ATR-imaging experimental set up, distances >400µm away from the interface could not be measured. Differences were observed in the distribution and the number of particles between the pH 1.5 and 7 datasets suggesting that particles at pH 1.5 are moving a greater distance relative to the interface in comparison to those particles present in the pH 7 environment within the same timeframe. A two-way ANOVA determined that there was a statistically significant difference in the distance travelled by the particles in the pH 1.5 and 7 environments after 58 minutes ($p < 0.05$, $n = 5$). This is most likely attributable to the low solubility of IT at higher pH impacting on the water uptake and swelling capacity of the tablet in comparison to that at pH 1.5. For reference, the solubility of IT at pH 7 is reported to be 1 ng/ml and the solubility at pH 1.5 is 4 µg/ml [24].

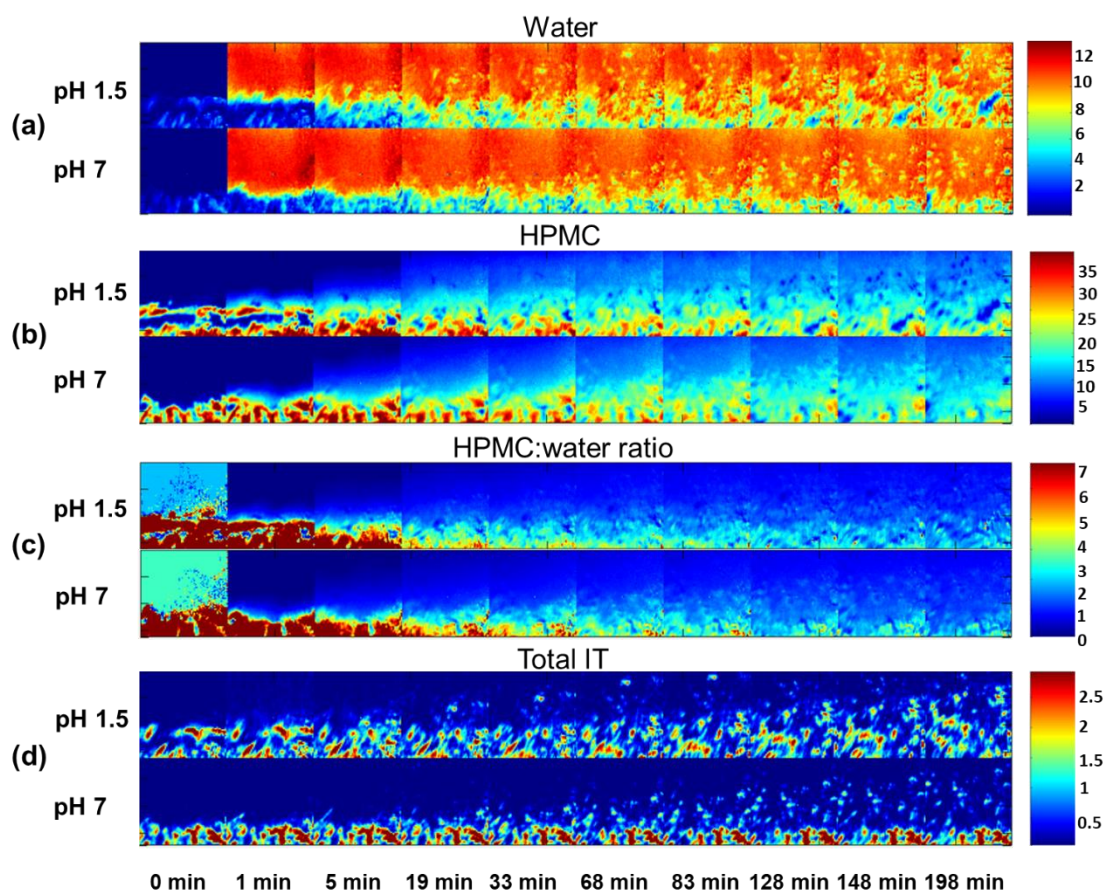


Fig. 5: ATR-FTIR peak area integration images over hydration period, showing: (a) distribution of water; (b) distribution of HPMC; (c) HPMC:water peak area ratio images, showing HPMC gel layer evolution for pH 1.5 and 7; (d) distribution of total IT.

We propose that as IT has much greater solubility at pH 1.5 it therefore will dissolve out of the matrix, effectively leaving a more “porous” structure than that observed at pH 7. This more porous matrix clearly has different expansion properties upon hydration as evidenced by the different outward IT particle translocation. Differences in the expansion properties were not observed in the placebo. Ultimately, monitoring actual drug particle movement by ATR-FTIR imaging, for a compound that shows pH dependent solubility, reveals more information pertaining to the nuances of the mechanism of drug release when compared to methods lacking chemical specificity, such as optical microscopy, to track glass beads.

3.5 Investigating the nature of IT particles within different pH environments

Infrared spectra were extracted across the central line of the highlighted particles in the images obtained after 28 minutes at pH 1.5 and pH 7, to determine if changes in particle mobility were linked to changes in the IT chemistry (Fig. 6d and 6e). The infrared spectra from the translocated particles were shown to be IT rich, although evidence of water and HPMC was also observed at both pH. Interestingly, the particle at pH 7 shows a greater intensity of HPMC across the particle in comparison to that at pH 1.5 as the edge of the diffusion front will be in different places due to the pH effect on IT solubility. Consequently, particles monitored will be located within different evolving fronts (swelling and diffusion) [1] [3] [4] depending on the pH.

As the tablet hydrates, the polymer chains start to relax creating the swelling front [32], this and the diffusion fronts move out further as the tablet continues to hydrate, translocating any undissolved particles inside the diffusion front with them.

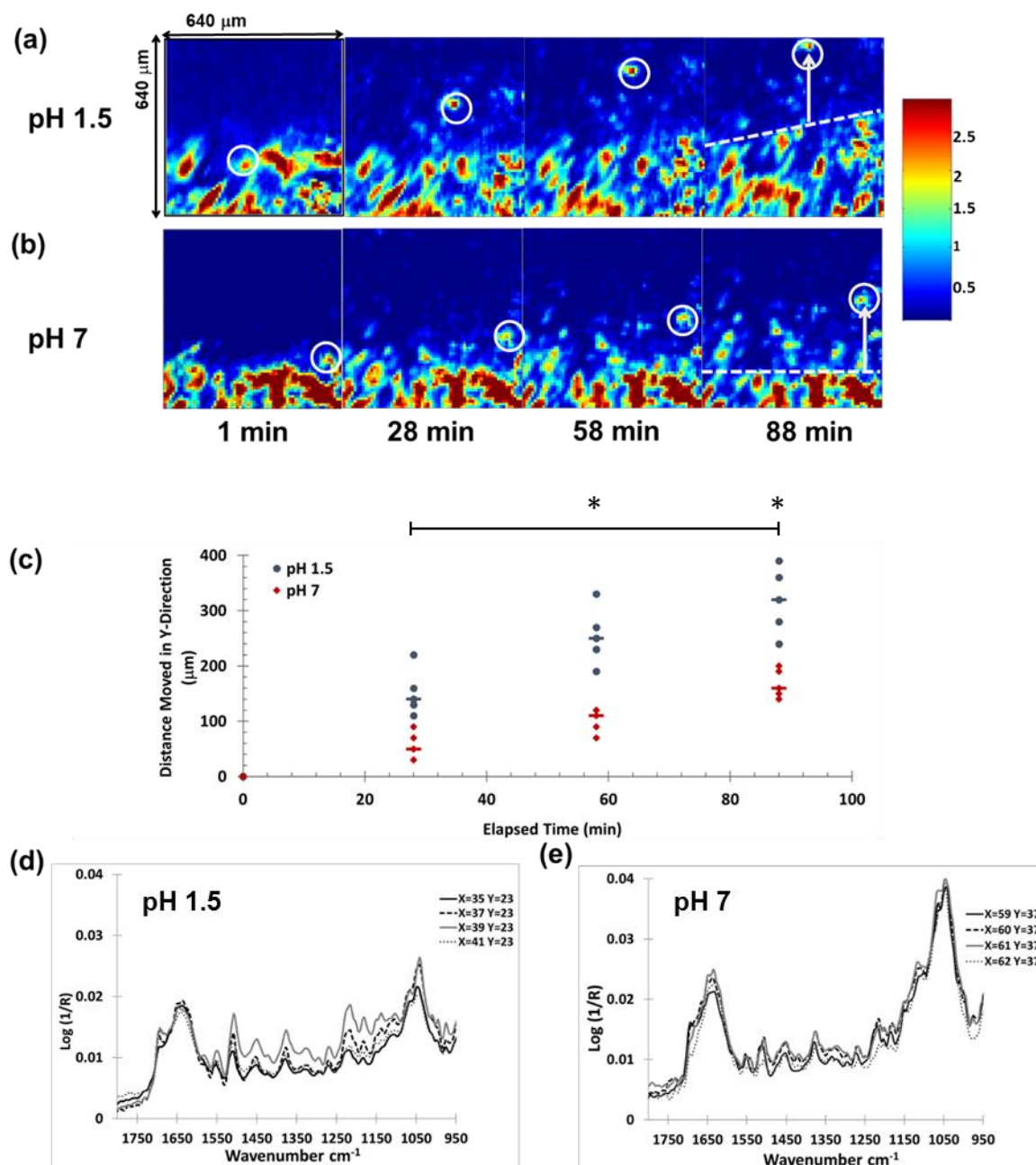


Fig. 6: ATR-FTIR images tracking an IT particle at selected time points at (a) pH 1.5 and (b) pH 7 (interface indicated by dashed white line in last pane), (c) Plot showing movement of 5 discrete particles at each pH over time ($p < 0.05$), FTIR spectra from selected pixels across the IT particle, showing that the particles are IT rich at the 28 minute time-point for (d) pH 1.5 and (e) pH 7.

3.6 Characterisation of the different forms of IT

FTIR is sensitive to molecular structure, therefore it is reasonable to assume that spectroscopic differences will be associated with the different forms of IT (ionised/ non-ionised form). For the images generated here, showing the distribution of IT in Fig.5d and Fig. 6a and b, the $\nu(\text{C}=\text{C}) \sim 1510 \text{ cm}^{-1}$ was used as the spectroscopic marker for IT. However, this band is present in both the ionised and un-ionised forms therefore it only shows the distribution of total IT. In order to ascertain that IR was sensitive to the different forms of IT, ATR-FTIR spectra were collected from IT salts (mono and dihydrochloride) prepared following procedures outlined previously [24][33]. Clear differences were observed between spectra obtained from the free base and IT salts, predominantly in the C-H stretching region. The free base form exhibits a strong band at 2821 cm^{-1} associated with CH symmetric stretching vibrations of the methyl group (Fig.7a) which disappears when the drug is ionised. Therefore the 2821 cm^{-1} band was used to generate peak area distribution images to show changes in IT chemistry over the course of the hydration period (Fig.7b). A greater intensity of undissolved free base is observed in the tablet core (towards the bottom of the image) for the high pH medium over the duration of the experiment. In contrast for the low pH environment, the intensity of the free base reduces rapidly as it starts to partially ionise, as expected with IT being more soluble at low pH. From this we can surmise that the IT is predominantly in the free base form in the images at the early time points at both pH 1.5 and pH 7. However IT remains in the free base form for the duration of the experiment behind the swelling front, with a small number of undissolved particles extending towards the diffusion front at pH 7.

Conversely, at pH 1.5 IT is predominantly in the ionised form at later time points, as illustrated by the loss of the free base (Fig. 7b), extending through to the outer edge of the diffusion front most probably due to improved solubility. A more detailed interrogation of the changes in chemistry of IT during the dissolution process can be performed by comparison of the infrared data extracted from the lowest 6 rows of pixels in these images. Binning the spectra within the pixels of the lowest six rows from images at 0, 33 and 198 minutes at both pH, it was possible to generate average spectra with sufficient S/N to elucidate differences in the IT chemistry between systems (Fig. 7c). It was observed that over the course of the dissolution experiment performed at pH 1.5 there was a subtle reduction in the intensity of the 2821 cm^{-1} band and a shift to higher wavenumber of the 2925 cm^{-1} band over time, which was indicative of a partial transformation of IT from the free base to the monohydrochloride form, shown more clearly in Figure 7d. Whereas at pH 7, there is no reduction in the intensity of the 2821 cm^{-1} band indicating that at pH 7, the IT remains in the free base form, with an associated lower solubility.

ATR-FTIR imaging studies provide a direct understanding how the low solubility pH-dependent drug, with a pKa in the physiological range, changes during the dissolution process. Following matrix swelling and expansion whilst tracking undissolved drug particles, in the way previous workers have tracked glass beads [4] it was possible to directly observe the relationship between particle translocation, drug solubility, ionisation state and distribution across the hydrated matrix at different media pHs. These factors will be important to drug release kinetics at different pH values.

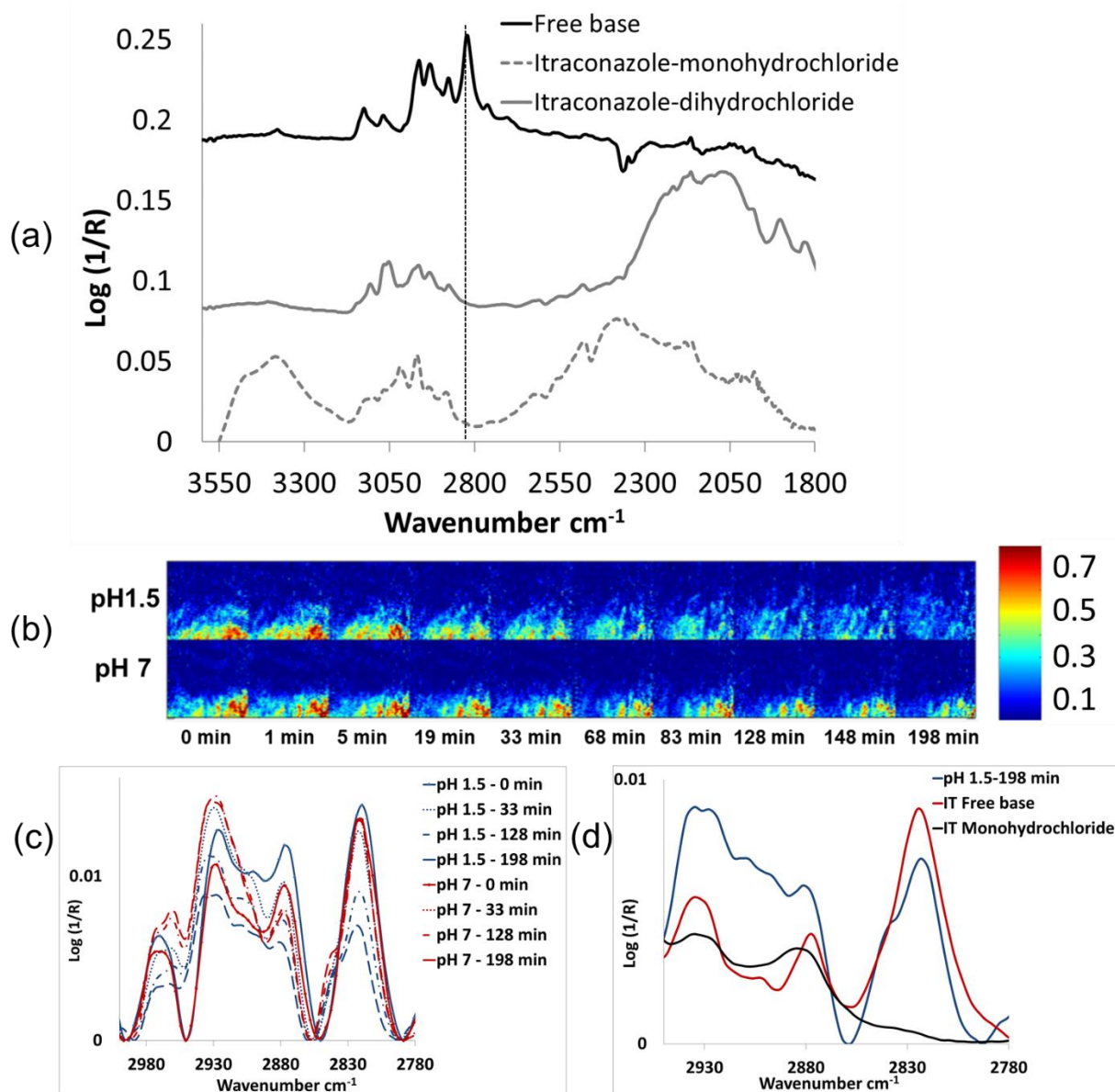


Fig. 7: (a) Average ATR-FTIR imaging spectra obtained from IT free base, IT monohydrochloride and IT dihydrochloride with dotted line indicating $\nu_s(\text{CH})$ at 2821 cm^{-1} . (b) ATR-FTIR peak area integrated images generated using band at 2821 cm^{-1} . (c) average ATR-FTIR imaging spectra highlighting $\nu(\text{CH})$ at 0, 33 and 198 minute timepoints for 20%w/w IT loaded tablets at pH 1.5 and 7. (d) average ATR-FTIR imaging spectra obtained from IT free base, IT monohydrochloride and 198 minute timepoint for 20%w/w IT loaded tablet at pH 1.5.

3.7 Physical swelling kinetics- radial and axial swelling results on 20%w/w IT loaded tablets

To supplement the ATR-FTIR data a series of swelling experiments were performed on both IT loaded and placebo tablets at pH 1.5 and pH 7. Examples of the optical images obtained from the placebo and 20% w/w IT loaded tablets for the 0 and 180 minute timepoint at pH 1.5 and 7 for the radial and axial measurements are shown in S_Fig. 4, S_Fig.5, S_Fig 7 and S_Fig.8. The results obtained from the swelling measurements confirmed that the swelling of placebo HPMC tablets was independent of pH, however there were a distinct difference in swelling behaviour of the 20% w/w IT loaded tablets in the different pH environments (Fig. 8). A greater degree of swelling was observed at pH 1.5 over the period of the hydration. Statistical analysis was carried out on the 30, 60, 90, 150 and 180 minute time point data using a two-way ANOVA to determine if there is a significant difference in both axial and/or radial swelling between tablets in the pH 1.5 and 7 environments. The results indicate that no statistically significant difference was observed at the 30-minute time-point, however a significant difference ($p < 0.05$) was observed for the subsequent time points analysed. Statistical analysis was also carried out on the placebo data at the same time points, however no significant difference was found for either the axial or radial dimensions between the pH environments (S_Fig. 6). These findings are in agreement with the FTIR-ATR imaging data presented earlier and support the hypothesis that the reduced swelling capacity of the IT loaded tablets at pH 7, leads to a reduction in the translocation of IT particles in the diffusion layer and consequently, along with the poor solubility of IT under these conditions, results in a retardation of IT release from these tablets.

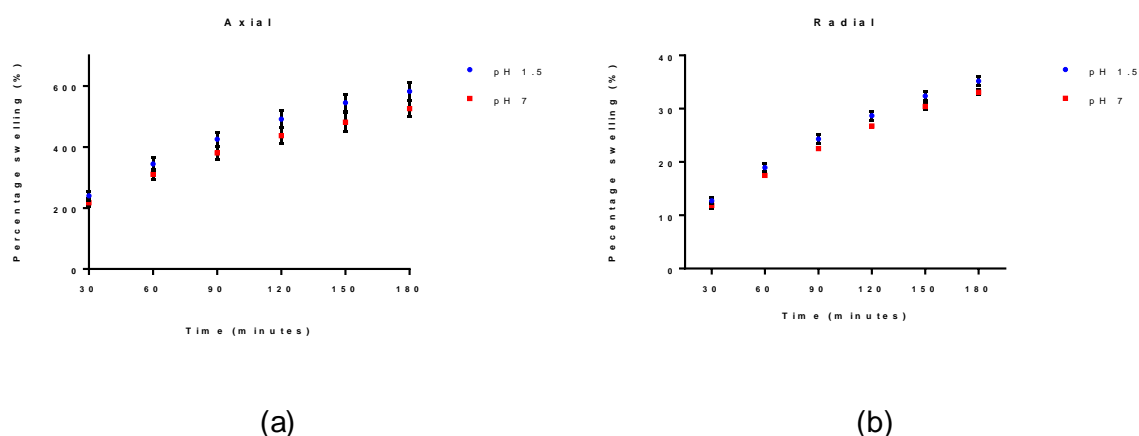


Fig. 8: Percentage swelling data obtained from 20% w/w IT loaded tablets from (a) axial (b) radial measurements

4 Conclusions

This work highlights the value of utilising ATR-FTIR imaging to elucidate factors affecting the release of a pH-dependent, poorly-soluble drug from a hydrophilic matrix. This approach permits an understanding of the within-matrix dynamics of the drug and shows that although evidence of particle translocation was observed in both pH 1.5 and 7 environments, drug mobility was very different between the two.

Using ATR-FTIR imaging to follow matrix swelling and expansion and track undissolved drug particles in the way previous workers have tracked glass beads [4], it was possible to observe the changing chemical nature of the drug as a particle moved within the diffusion front. At pH 7 the drug remained in the free base form, which is poorly-soluble and therefore largely stayed within the core and the swelling front. At pH 1.5 however, the IT was partially ionised, becoming more soluble and was able to migrate into the diffusion front and eventually out into the surrounding medium. The IT containing tablets exposed to the low pH medium show a higher swelling rate and greater overall percentage swelling in comparison to those exposed to the pH 7 environment. No significant differences in the swelling behaviour were observed for placebo tablets.

Therefore, we conclude that differential drug solubility observed across the pH range is not the sole reason for different release rates within different pH environments. Additionally, the presence of non-dissolved drug negatively impacts upon matrix swelling resulting in translocated free base drug particles being in the swelling front at pH 7 and partially ionised drug particles in the diffusion front at pH 1.5. In combination, differences in solubility of the drug and swelling of the matrix affect the rate and percentage drug release at the two different pHs.

Acknowledgements

The authors would like to thank Sheffield Hallam University for providing the funding and Bristol-Myers Squibb for supporting the project and kindly donating the materials. The authors thank the valuable technical assistance offered by Dr Natalka Johnson, Gary Robinson, Paul Allender and Laura McLaughlin.

Supporting Information

NIR data for quantification of tablet composition, Raman data to ascertain IT distribution, in vitro dissolution data and axial and radial swelling data supplied as Supporting Information.

References

- [1] P. Timmins, D. Desai, W. Chen, P. Wray, J. Brown and S. Hanley, "Advances in mechanistic understanding of release rate control mechanisms of extended-release hydrophilic matrix tablets," *Therapeutic delivery*, vol. 7, no. 8, p. 553–572, 2016.
- [2] D. A. Alderman, "A review of cellulose ethers in hydrophilic matrices for oral controlled-release dosage forms.," *International Journal of Pharmaceutical Technology and Product Manufacture*, vol. 5, pp. 1-9, 1984.
- [3] P. Colombo, R. Bettini, G. Massimo, P. L. Catellani, P. Santi and N. Peppas, "Drug diffusion front movement is important in drug release control from swellable matrix tablets," *Journal of Pharmaceutical Sciences*, vol. 84, no. 8, p. 991–997, 1995.
- [4] R. Bettini, P. L. Catellani, P. Santi, G. Massimo, N. A. Peppas and P. Colombo, "Translocation of drug particles in HPMC matrix gel layer: effect of drug solubility and influence on release rate," *Journal of Controlled Release*, vol. 70, no. 3, p. 383–391, 2001.
- [5] J. Alder, A. Jayan and C. Melia, "A Method for Quantifying Differential Expansion within Hydrating Hydrophilic Matrixes by Tracking Embedded Fluorescent Microspheres," *Journal of Pharmaceutical Sciences*, vol. 88, no. 3, pp. 371-377, 1999.
- [6] J. L. Ford, "Design and Evaluation of Hydroxypropyl Methylcellulose Matrix Tablets for Oral Controlled Release: A Historical Perspective," in *Hydrophilic Matrix Tablets for Oral Controlled Release*, P. Timmins, S. R. Pygall and D. R. Melia, Eds., New York, AAPS Advances in the Pharmaceutical Sciences Series, vol 16. Springer, 2014, pp. 17-51 .
- [7] K. Asare-Addo, M. Levina , A. R. Rajabi-Siahboomi and A. Nokhodchi, "Effect of ionic strength and pH of dissolution media on theophylline release from hypromellose matrix tablets—Apparatus USP III, simulated fasted and fed conditions," *Carbohydrate Polymers*, vol. 86, no. 1, pp. 85-93, 2011.
- [8] G. S. Bajwa, K. Hoebler, C. Sammon, P. Timmins and C. D. Melia, "Microstructural imaging of early gel layer formation in HPMC matrices," *Journal of Pharmaceutical Sciences*, vol. 95, no. 10, pp. 2145-2157, 2006.
- [9] U. Mikac, A. Sepe, J. Kristl and S. Baumgartner, "A new approach combining different MRI methods to provide detailed view on swelling dynamics of xanthan tablets influencing drug release at different pH and ionic strength," *Journal of Controlled Release*, vol. 145, no. 3, pp. 247-256, 2010.

- [10] X. Ming Xu, Y. M. Song, Q. N. Ping, Y. Wang and X. Y. Liu, "Effect of Ionic Strength on the Temperature-Dependent Behavior of Hydroxypropyl Methylcellulose Solution and Matrix Tablet," *Journal of Applied Polymer Science*, vol. 102, no. 4, pp. 4066-4074, 2006.
- [11] P. Timmins, A. M. Delargy and J. R. Howard, "Optimization and Characterization of a pH Independent Extended-Release Hydrophilic," *Pharmaceutical Development and Technology*, vol. 2(1), pp. 25-31, 1997.
- [12] T. Vasconcelos, B. Sarmiento and P. Costa, "Solid dispersions as strategy to improve oral bioavailability of poor water soluble drugs," *Drug Discovery Today*, vol. 12, no. 23-24, p. 1068-1075, 2007.
- [13] D. J. Good, R. Hartley, N. Mathias, J. Crison, G. Tirucherai, P. Timmins, M. Hussain, R. Haddadin, O. Koo, F. Nikfar and N. K. Fung, "Mitigation of Adverse Clinical Events of a Narrow Target Therapeutic Index Compound through Modified Release Formulation Design: An in Vitro, in Vivo, in Silico, and Clinical Pharmacokinetic Analysis," *Molecular Pharmaceutics*, vol. 12, p. 4434-4444, 2015.
- [14] A. T. Serajuddin, "Salt formation to improve drug solubility," *Advanced Drug Delivery Reviews*, vol. 59, no. 7, p. 603-616, 2007.
- [15] A. Ewing, G. Clarke and S. G. Kazarian, "Stability of indomethacin with relevance to the release from amorphous solid dispersions studied with ATR-FTIR spectroscopic imaging," *European Journal of Pharmaceutical Sciences*, vol. 60, p. 64-71, 2014.
- [16] K. Chan and S. Kazarian, "Visualisation of the heterogeneous water sorption in a pharmaceutical formulation under controlled humidity via FT-IR imaging," *Vibrational Spectroscopy*, vol. 35, no. 1-2, pp. 45-49, 2004.
- [17] A. V. Ewing and S. G. Kazarian, "Recent advances in the applications of vibrational spectroscopic imaging and mapping to pharmaceutical formulations," *Spectrochimica Acta Part A: Molecular and Biomolecular Spectroscopy*, vol. 197, pp. 10-29, 2018.
- [18] K. Punčochová, A. V. Ewing, M. Gajdošová, N. Sarvašová, S. G. Kazarian, J. Beránek and F. Štěpánek, "Identifying the mechanisms of drug release from amorphous solid dispersions using MRI and ATR-FTIR spectroscopic imaging," *International Journal of Pharmaceutics*, vol. 483, no. 1-2, p. 256-267, 2015.
- [19] S. G. Kazarian and K. L. Chan, "Applications of ATR-FTIR spectroscopic imaging to biomedical samples," *Biochimica et Biophysica Acta*, vol. 1758, p. 858-867, 2006.
- [20] P. S. Wray, G. S. Clarke and S. G. Kazarian, "Application of FTIR Spectroscopic Imaging to Study the Effects of Modifying the pH Microenvironment on the Dissolution of Ibuprofen from HPMC Matrices," *Journal of Pharmaceutical Sciences*, vol. 100, no. 11, pp. 4745-4755, 2011.

- [21] J. Van der Weerd and S. G. Kazarian, "Combined approach of FTIR imaging and conventional dissolution tests applied to drug release," *Journal of Controlled Release*, vol. 98, no. 2, p. 295–305, 2004.
- [22] H. Hifumia, A. V. Ewing and S. G. Kazarian, "ATR-FTIR spectroscopic imaging to study the drying and dissolution of pharmaceutical polymer-based films," *International Journal of Pharmaceutics*, vol. 515, no. 1-2, p. 57–68, 2016.
- [23] A. V. Ewing, G. S. Clarke and S. G. Kazarian, "Attenuated total reflection-Fourier transform infrared spectroscopic imaging of pharmaceuticals in microfluidic devices," *Biomicrofluidics*, vol. 10, no. 2, 2016.
- [24] T. Tao, Y. Zhao, J. Wu and B. Zhou, "Preparation and evaluation of itraconazole dihydrochloride for the solubility and dissolution rate enhancement," *International Journal of Pharmaceutics*, vol. 367, no. 1-2, p. 109–114, 2009.
- [25] S. R. Pygall, S. Kujawinski, P. Timmins and C. D. Melia, "The suitability of tris(hydroxymethyl) aminomethane (THAM) as a buffering system for hydroxypropyl methylcellulose (HPMC) hydrophilic matrices containing a weak acid drug," *International Journal of Pharmaceutics*, vol. 387, p. 93–102, 2010.
- [26] K. C. Gordona and C. M. McGoverin, "Raman mapping of pharmaceuticals," *International Journal of Pharmaceutics*, vol. 417, p. 151–162, 2011.
- [27] FDA U.S. Food and Drug Administration, "Dissolution Methods-itraconazole," [Online]. Available: https://www.accessdata.fda.gov/scripts/cder/dissolution/dsp_SearchResults.cfm. [Accessed 19 July 2019].
- [28] X. Yin, L. S. Daintree, S. Ding, D. M. Ledger, B. Wang, W. Zhao, Q. Jianping and W. Wu, "Itraconazole solid dispersion prepared by a supercritical fluid technique: preparation, in vitro characterization, and bioavailability in beagle dogs," *Drug Design, Development and Therapy*, vol. 2015:9, p. 2801–2810, 2015.
- [29] J. Peeters, P. Neeskens, J. P. Tollenaere, P. V. Remoortere and M. E. Brewster, "Characterization of the Interaction of 2-Hydroxypropyl- β cyclodextrin With Itraconazole at pH 2, 4, and 7," *Journal of Pharmaceutical Sciences*, vol. 91, no. 6, p. 1414–1422, 2002.
- [30] J. L. Ford, K. Mitchell, P. Rowe, D. J. Armstrong, P. N. Elliott, C. Rostron and J. E. Hogan, "Mathematical modelling of drug release from hydroxypropylmethylcellulose matrices: effect of temperature.," *International Journal of Pharmaceutics*, vol. 71, no. 1-2, p. 95–104, 1991.
- [31] P. Colombo, R. Bettini, P. Santi, A. De Ascentiis and N. A. Peppas, "Analysis of the swelling and release mechanisms from drug delivery systems with emphasis on drug solubility and water transport," *Journal of Controlled Release*, vol. 39, no. 2-3, pp. 231-237, 1996.

- [32] M. U. Ghori and B. R. Conway, "Hydrophilic Matrices for Oral Control Drug Delivery," *American Journal of Pharmacological Sciences*, vol. 3, no. 5, pp. 103-109, 2015.
- [33] H. Bagavatula, S. Lankalapalli, V. Tenneti, N. Beeraka and B. Bulusu, "Comparative Studies on Solubility and Dissolution Enhancement of Different Itraconazole Salts and Their Complexes," *Advances in Pharmacology and Pharmacy*, vol. 2, no. 6, pp. 85-89, 2014.